Water Harvesting Research, 2017, 2(1): 24-36
DOI: 10.22077/jwhr.2017.593
www.jwhr.birjand.ac.ir
P-ISSN: 2476-6976, E-ISSN: 2476-7603

Simulation of flow pattern in intake by using a numerical model

Reza Babagoli Sefidkoohi[a], Ali Shahidi[b*], Yousef Ramezani [c],Mehdi Kahe[d]

[a] M.Sc. Graduate, Water Engineering Department, University of Birjand.

[b] Associate Professor, Water Engineering Department, University of Birjand.

[c] Assistant Professor, Water Engineering Department, University of Birjand.

[d] Ph.D. Graduate, Hydraulic Structures Department, Shahid Chamran University of Ahvaz.

[*] Corresponding author, E-mail address: ashahidi@birjand.ac.ir

Received: 8 May 2016 / Accepted: 7 June 2017

Abstract

Lateral intake is a structure constructed next to a main channel to divert part of the flow within the channel. The separated area of the flow in the entrance of intake channel has no effect on flow discharge while reduces the effective cross-sectional area of the intake, as well as the bed load, which enters the intake due to low velocity flow deposits in this area. Thus, knowing the dimensions of the separated area at the intake channel entrance is particularly important. In this study, flow separation zone was calculated at the intake entrance of 90 degree in three depths of 3, 6, and 12 cm from the bottom of the channel for discharge ratios of 0.2 and 0.4, 0.6 and 0.8 in five turbulence models using three-dimensional Flow-3D model. In order to determine the accuracy of the model in predicting the dimensions of the separated areas, the obtained results were compared with the results of the physical model. Streamlines were drawn and dimensions of the separated areas were determined. In comparing results between the laboratory observations and the predicted ones by numerical model, Reynolds Normal Group model (RNG) had better predictions, with a correlation coefficient of 0.97, root mean square error of 3.16, and a mean absolute error of 2.3 cm, than other turbulence models.

Keywords: *Intake 90°, Flow pattern, Turbulence models, Flow-3D numerical model, Laboratory observations.*

1. Introduction

In designing hydraulic structures, determining a branched flow from a main channel to the lateral channel is of high importance. Pressure changes at the intake are such that the pressure declines in the internal intake zone and increases within the external intake zone. These high and low pressure areas are a result of changes in water surface levels of the intake. Divided size of the flow in the main channel is what determines the harvested amount through the diversion channel. A balance between longitudinal pressure gradient, shear forces, and centrifugal forces leads to the formation of secondary flow in a clockwise direction within the external wall of diversion channel, which is a formation mechanism similar to the formation of secondary flow in the bends. Figure.1 depicts a schematic of the three-dimensional flow pattern in a lateral intake. This secondary flow along with the separated area within the inner wall of diversion channel (area A in figure 1) creates a completely complex and three-dimensional flow.

This separated area is dependent on the cross-sectional shape and is influential on the diversionary relative discharge. In this area of the flow, fluid particles at a distance from the wall are in motion around themselves. In fact, this area of lateral intake has no influence on the amount of flow discharge. In other words, the separation area reduces the effective cross section of the intake.

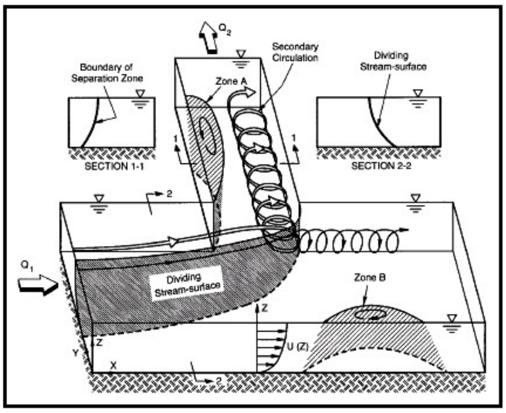

Fig. 1. The flow pattern in a lateral intake (Neary & Odgaard, 1993)

In one hand, due to the curvature of flow divider surface (Section 2-2) a main part of the bed load enters into the intake through vortex flow deposited in this area caused by low-velocity flow. Thus, knowing the dimensions of a separated area in the lateral intake is highly important. The involved factors in the formation of flow pattern in such fields are inlet flow discharge, ratio of diversionary discharge, relative width of main and branched channels, depth of flow to channel width ratio, and bed roughness of main channel (8).

Neary & Odgaard (1993) conducted laboratory studies on hydraulic flow in the 90 degree intake. The main channel was built with two smooth and rough beds, wherein flow pattern, flow separation line, stagnation zone, and vortices forming area were analyzed at the intake (9). Issa & Oliveira (1994), for the first time, investigated numerical modeling of three-dimensional turbulent flow pattern.

These two researches solved the Navier-Stokes equations with time averaging through finite volume method and applying turbulence model k-Ɛ with standard wall function and used over 30000 nodes.

Neary & Sotiropoulos (1996) examined the layer flow sample in 90-degrees intake using a three-dimensional numerical model (10). Shettar & Murthy (1996) simulated the turbulent flow pattern in 90 degrees intake by preparing an averaged two-dimensional model in depth, which was fastened with k-ε turbulence model along with the standard wall function (13). Kasthuri & Pundarikanthan (1987) carried out some researches about the dimensions of the separated area and flow separation in a 90-degrees intake. The results indicated that as discharge increased, the length and width of the separated area at the intake decreases (6). Neary et al. (1999) offered a three dimensional model using RAN equations and k-ω turbulence model. The comparisons of velocity profile with laboratory observations showed that the model has a high accuracy (8). By providing a three dimensional model and comparing it with laboratory results, Ramamurthy et al. (2007) indicated a good agreement between velocity profiles, separation zone, water depth, and the secondary flow. They used the two-equation turbulence model k-ω in order to calculate the Reynolds stresses. They then used a three-dimensional model for analyzing the spiral vortex, which was formed at the intake and it was found that by increasing discharge ratio, vortex power will increase as well, while causing a reduction at downstream of the intake (11).

Seyedian & Shafai bajestan (2009) studied flow pattern in a lateral intake for two modes of main channel with steep and vertical walls using a SSIIM 2 three-dimensional model. In the calibration stage, they selected RNG and k-ε model as the best turbulence model. The results showed that the formation of slopes caused modified flow pattern such that the flow channel width in the bed decreased and then increased on the surface. They also depicted that a flow tube cross-sectional area decreases compared to the vertical wall (1).

Gohari (2012) conducted laboratory experiments of flow separation line at the intakes and its relation to controlling the sediment. In this research, the effect of spur dike structures and vanes was examined on the flow separation line at the intakes. Attention was also paid to the method of changing the flow separation line, which was in direct relation with sediments entrance into the intake. Results indicated that vanes can affect the flow lines and the flow separation line through creating secondary flow. Although with simultaneous application of the vanes and the spur dike structure, the flow separation line development decreased in the bed of the main channel. However, local scouring must be considered in front of intake due to reinforcing the flow velocity (4).

Tataroglu & Özgen (2014) numerically investigated the vortex area formation formed in a tank in dewatering from reservoir with pipe using Flow-3D model and then compared the results with laboratory results. Critical submerged depth, which is essential for the formation of vortices in the reservoir surface, was determined for each experiment (12).

With respect to the limitations of using physical models, numerical models have become widely used due to their ease of use. An important problem in numerical models is the accuracy of their results.

The only way in which the researcher can appropriately judge the accuracy of the numerical solution outcomes is by preparing various laboratory models, their assessment, and the comparison with each other. In this research the length and width of the separated area in 90-degrees intake was calculated with flow-3D model for various discharge ratios and five turbulence models. Results were then compared with the observations of physical models.

The discharge ratio is defined as $r = \frac{Q_2}{Q_1}$, where Q_2 is the discharge at the intake channel and Q_1 is the total discharge in the main channel. For example, if 80% of the total discharge is diverted from the main channel, discharge ratio would be 80 percent or 0.8.

So far researches have focused on numerical simulation of flow pattern at the intakes with Flow-3D model and finding the best turbulence models to predict the length and width of the separated area at different levels of water depth. In this regard, the present study focuses on comparing laboratory observations of the separated areas at different depths and Flow-3D numerical model results in the 90-degrees intake.

2. Materials and Methods

Physical model

In conducting this research, the results of the physical model obtained from the studies of Karami Moghaddam (2008) and Karami Moghaddam and Keshavarzi (2008) were used (2 and 3). The main and the intake channels had 50 and 25 cm width and 40 cm height, respectively. The main channel slope was considered as 0.003 and intake channel slope was zero. The discharge range varied from 15 to 35 lit/sec for several discharge ratios. The range of the Froud numbers was between 0.15 and 0.4 lit/ sec.

FLOW-3D numerical model

FLOW-3D model is an effective tool in the field of Computational Fluids Dynamics (CFD). This model is capable of three-dimensional analysis of the flow field and has a vast practical range including issues related to fluids. FLOW-3D model includes many physical patterns such as shallow waters, viscosity, cavitation, turbulence, porous environments, etc. This model is functional in areas such as casting, process engineering, hydraulics, aerospace, marine sciences, oil, gas, etc.

Experimental studies of turbulent flow characteristics were very time-consuming and costly and the level of the obtained information was low.

Considering the random nature of particles' movement, fluid masses, and their extra irregularities in turbulent flow, studying this type of flow theoretically is difficult and even impossible. The existing models for solving turbulences are not able to examine turbulences with unlimited details. However, they provide valuable information from an engineering point of view.

The base of the governing equations for solving laminar and turbulent flows were similar and Navier-Stokes and continuity equations were used. The only difference is that in order to solve turbulent flow, Navier-Stokes equations must be time averaging, ergo the emergence of some extra terms in the Navier-Stokes equations interpreted as stress values and called turbulence stresses (Reynolds stresses).

Turbulence models were used for solving additional terms which appeared in Navier-Stokes equations.

In order to analyse turbulent flows, first, flow moment properties (for example, components of velocity and pressure) were analysed in a context of mean value and a fluctuating value:

$$u_i = \bar{u}_i + u'_i \qquad (1)$$

$$p = \bar{p} + p' \qquad (2)$$

where the parameters $\bar{u}_i$ and $\bar{p}$ are; time-averaged velocity and pressure values, respectively, and parameters u'_i and p' present the amount of their fluctuations.

The above analysis aims to study turbulent flows through Navier-Stokes equations. As for the study of turbulent flows using ordinary form of Navier-Stokes equations, it is necessary to consider very small cell dimensions and time steps.

By placing relationships (1) and (2) in Navier-Stokes and continuity equations and by time averaging of achieved relations, the following equations were obtained:

Continuity:

$$\frac{\partial \bar{u}}{\partial x} + \frac{\partial \bar{v}}{\partial y} + \frac{\partial \bar{w}}{\partial z} = 0 \qquad (3)$$

Navier-Stokes:

$$\rho\left(\frac{\partial \bar{u}}{\partial t} + \bar{u}\frac{\partial \bar{u}}{\partial x} + \bar{v}\frac{\partial \bar{u}}{\partial y} + \bar{w}\frac{\partial \bar{u}}{\partial z}\right) = F_x - \frac{\partial \bar{p}}{\partial x} + \mu\Delta\bar{u} - \rho\left(\frac{\partial \overline{u'u'}}{\partial x} + \frac{\partial \overline{u'v'}}{\partial y} + \frac{\partial \overline{u'w'}}{\partial z}\right) \qquad (4)$$

$$\rho\left(\frac{\partial \bar{v}}{\partial t} + \bar{u}\frac{\partial \bar{v}}{\partial x} + \bar{v}\frac{\partial \bar{v}}{\partial y} + \bar{w}\frac{\partial \bar{v}}{\partial z}\right) = F_y - \frac{\partial \bar{p}}{\partial y} + \mu\Delta\bar{v} - \rho\left(\frac{\partial \overline{u'v'}}{\partial x} + \frac{\partial \overline{v'v'}}{\partial y} + \frac{\partial \overline{v'w'}}{\partial z}\right) \qquad (5)$$

$$\rho\left(\frac{\partial \bar{w}}{\partial t} + \bar{u}\frac{\partial \bar{w}}{\partial x} + \bar{v}\frac{\partial \bar{w}}{\partial y} + \bar{w}\frac{\partial \bar{w}}{\partial z}\right) = F_z - \frac{\partial \bar{p}}{\partial z} + \mu\Delta\bar{w} - \rho\left(\frac{\partial \overline{u'w'}}{\partial x} + \frac{\partial \overline{v'w'}}{\partial y} + \frac{\partial \overline{w'w'}}{\partial z}\right) \qquad (6)$$

The last terms on the right side of the time-averaged Navier-Stokes equations indicate the Reynolds stresses.

The only difference between the above equations and the typical form of Navier-Stokes equations is the addition of the related to Reynolds stresses. Turbulence models are aimed at finding the right solution for estimating the amount of this term.

In most turbulence models, Boussinesq theory is used for determining the Reynolds stresses. This hypothesis with the coefficient of eddy viscosity relates the Reynolds stresses to the velocity gradients.

$$\overline{u'_i u'_j} = v_t\left[\frac{\partial u_i}{\partial x_j} + \frac{\partial u_j}{\partial x_i}\right] \qquad (7)$$

$$\tau_{i,j} = \rho\overline{u'_i u'_j} = \mu_t\left[\frac{\partial u_i}{\partial x_j} + \frac{\partial u_j}{\partial x_i}\right] \qquad (8)$$

, where v_t and μ_t are kinematic and dynamic eddy viscosity, respectively and $\mu_t = \rho v_t$. Since the eddy viscosity was applied to estimate the turbulent stresses, it should be a function of turbulent flow characteristics.

There is doubt which says that the flow characteristics are most suitable for formulating μ_t with respect to the eddy viscosity dimension [m2/s]. The best selections could be the velocity and length scales.

Therefore, the following equation is represented for dynamic eddy viscosity:

$$\mu_t = C\rho v_t L \quad (9)$$

where C is a constant coefficient, ρ is the fluid density, v_t is velocity scale, and L is the length scale.

Types of turbulence models

Many turbulent models have been developed for simulating turbulent flows by various researchers. These models are based on the method of operation and therefore, the differential equations, which are used for turbulent quantities, will be divided into the categories of zero-equation models, models of one-equation, models of two- equation, models with stress equation, and models of simulating large eddies. In the following, a brief introduction of above models are presented.

1. Zero-equation model: in these models, differential equations are not used for determining turbulence quantities. These models are relatively simple and are formulated based on experimental and laboratory data. Some types of these models include; constant eddy viscosity, Prandtl mixing length model, and Prandtl free cutting layer model.

2. One -equation model: these models make use of a differential equation in terms of turbulence quantity k, where k is the turbulent kinetic energy which is defined by the following relationship:

$$k = \frac{1}{2}(u'^2 + v'^2 + w'^2) \quad (10)$$

Velocity scale (V_t) is defined as follows:

$$v_t = \sqrt{k} \quad (11)$$

Therefore, turbulence passives transform into k and l quantities. K can be determined by solving the Navier-Stokes equation for this parameter.

3. Two-equation model: the length scales in these models, unlike the one- equation model, are estimated without relying on empirical relationships. In these models, the turbulence quantities, which are extracted from solving differential equation, are used to estimate length and velocity scales. Some of these models include eddy viscosity, algebraic and non-linear Reynolds stress.

These models also incorporate another turbulence quantity estimated similar to the parameter k using Navier-Stokes equation. One of the defined quantities in these models is the quantity of turbulence waste or ε [m2/s3]. Ɛ quantity represents the length scale. In fact, the length scale represents the size of large vortices with kinetic energy transferring turbulence into fluid mass.

4. Models with stress equation: these models are based on Reynolds Normalized Groups (RNG). This approach includes statistical methods for extracting the averaged equations for turbulence quantities such as turbulence kinetic energy and its dissipation rate.

RNG model uses relations such as those available in the k-ε model. The difference is that constant coefficients in k-ε model, which are extracted experimentally, are calculated explicitly in the RNG model.

5. Large eddy simulation model: the main idea of this model is to directly calculate all turbulent structures computable using computational network and to estimate just those tiny structures that aren't computable.

For example, in analyzing the turbulence model using LES around a large building, in addition to the averaged stresses of wind, an estimation is obtainable from magnitude and standard deviation of maintained forces fluctuation from turbulent flow.

The simulation of turbulence is carried out in FLOW-3D using one of the five models with this software. The turbulence models used by the FLOW-3D include: Prandtl mixing length, turbulent kinetic energy equation, the two-equation of k-ε model, model of Reynolds Normalized Groups RNG, and Large Eddy simulation model.

Meshing and boundary conditions

In order to provide channel geometry, Auto CAD software was used. Initially, the geometries of the main channel and the intake were drawn using Auto CAD software according to the laboratory conditions, then were transformed into Stl format, which is operative in FLOW-3D software.

Model meshing can be implemented using perpendicular cube elements (or quadrilateral). It is recommended to use smaller cells in areas with high gradient. In regards to this point and considering the stability conditions of the numerical models, 1 cm meshing was used for z direction and 1 or 2 cm meshing were used in X and Y directions for various turbulence models.

Boundary condition of flow discharge and flow depth in X_{min}, X_{max}, and Y_{min} are the entrance of main channel, the outlet of main channel, and the outlet of intake, respectively. Y_{max} and Z_{min} include boundary conditions of rigid wall (Wall) and Z_{max}, which is the free surface of flow, includes the boundary condition of the applied symmetry. At the end of the simulation by FLOW-3D software, data were exported in TEXT format and entered into Tecplot software after being recalled in Excel software.

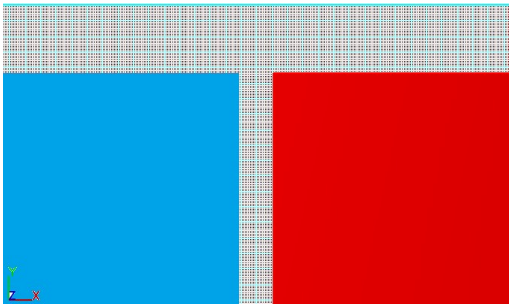

Fig.2. The mesh model

Drawing the streamlines

Using the obtained velocity components from Flow-3D model in the various areas of main and lateral intake and Tecplot software, streamlines were drawn for various turbulence models and different discharge ratios were sat heights of 3, 6 and 12 cm above the canal bed. The dimensions of the separated areas of flow were then determined.

Examples of streamlines are shown in Figures 3 to 17.

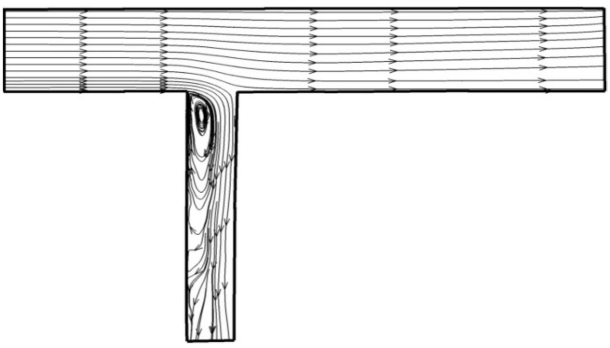

Fig. 3. RNG,0.2, 3 cm

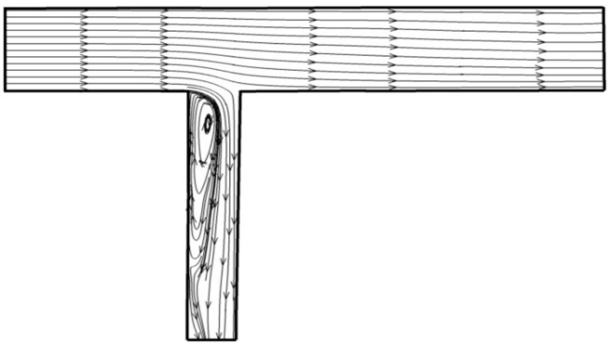

Fig. 4. RNG,0.2, 12 cm

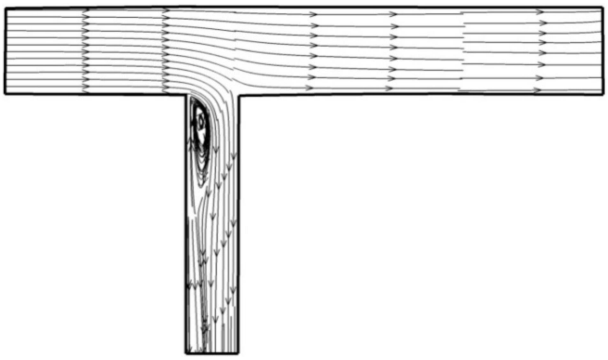

Fig. 5.RNG, 0.4, 3 cm

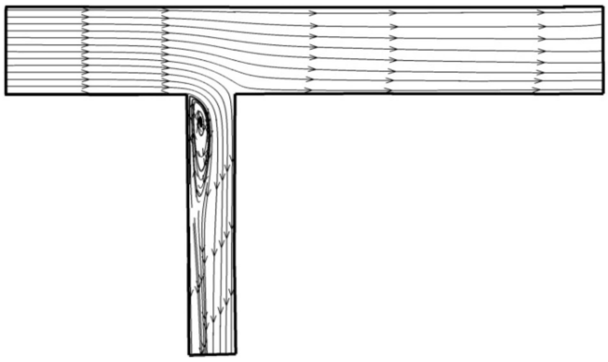

Fig. 6. RNG, 0.4, 12 cm

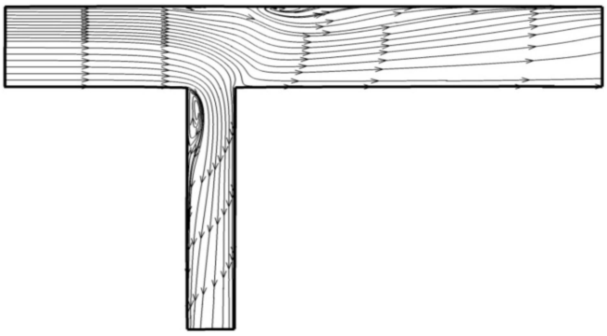

Fig. 7. RNG, 0.6, 3 cm

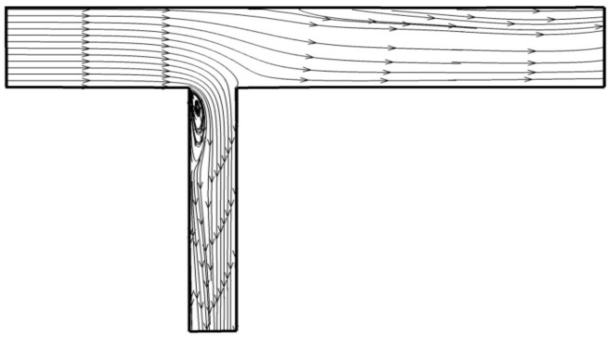

Fig. 8. RNG, 0.6, 12 cm

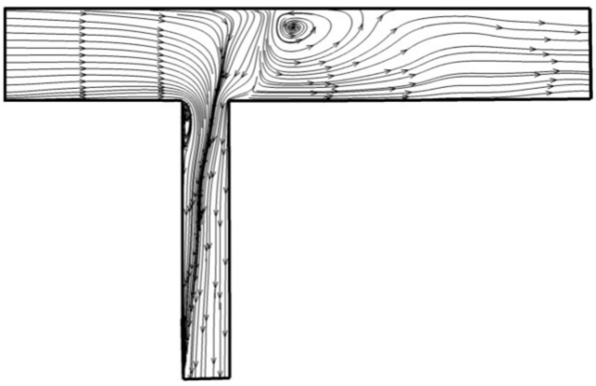

Fig. 9. RNG, 0.8, 3 cm

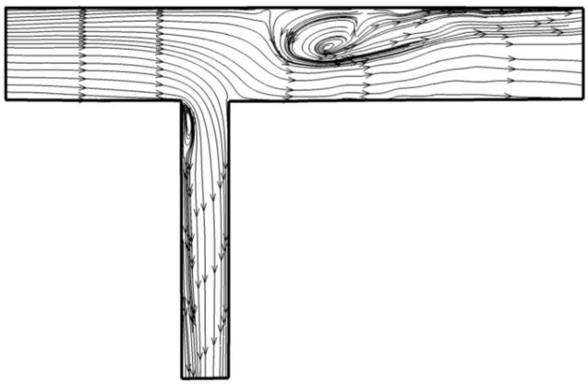

Fig. 10. RNG, 0.8, 12 cm

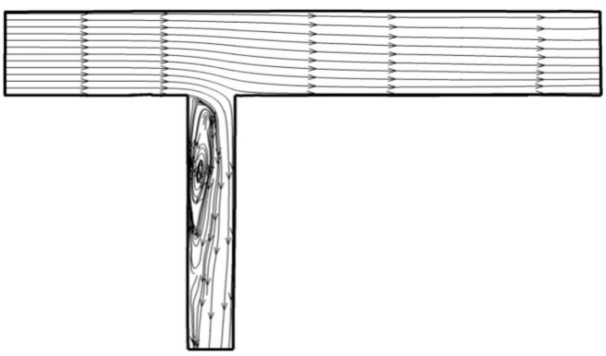

Fig. 11. K-ε, 0.2, 3 cm

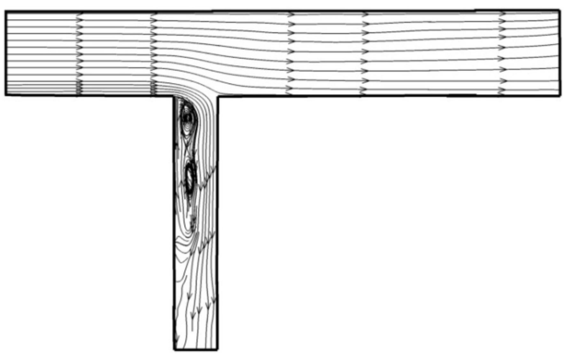

Fig. 12. K-ε, 0.2, 12 cm

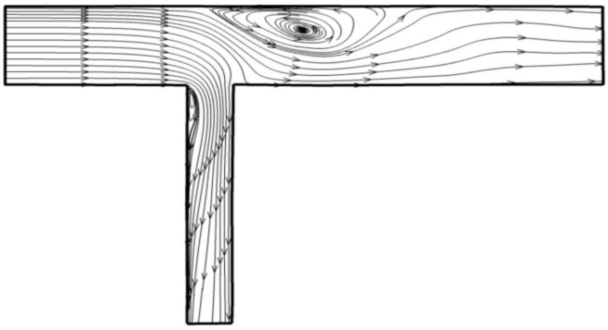

Fig. 13. K-ε,0.8, 3 cm

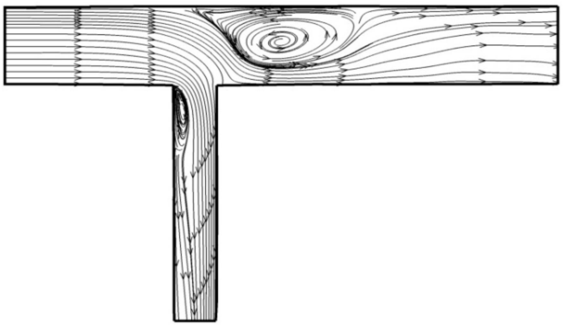

Fig. 14. K-ε, 0.8, 12 cm

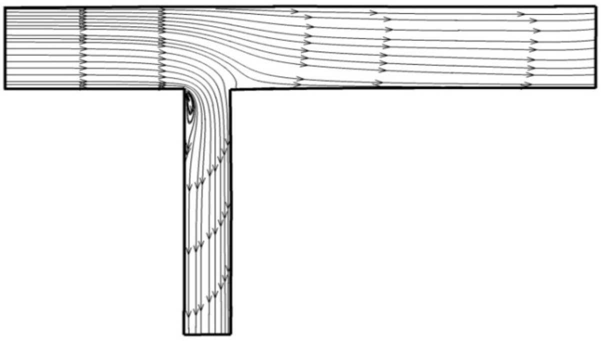

Fig. 15. Turbulent energy,0.6, 12 cm

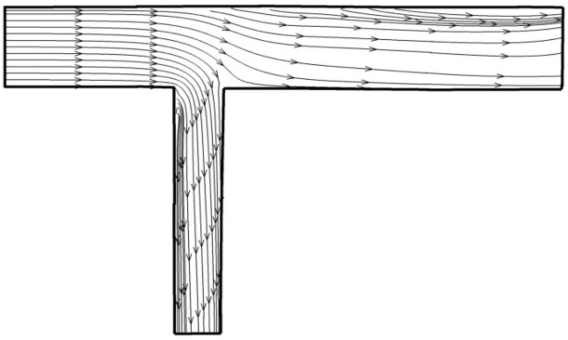

Fig. 16. Prandtl mixing length,0.6, 12 cm

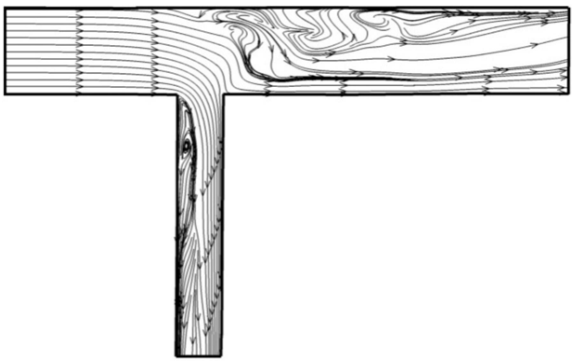

Fig. 17. Large eddy, 0.6, 12 cm

In order to find the best turbulence model amongst the numerical models for predicting the dimensions of the separated area, three statistical indexes of correlation coefficient, root mean square error, and mean absolute error were used. These statistical indices are formulated as:

$$R^2 = 1 - \frac{\sum_{i=1}^{n}(predicted\ value_i - measured\ value_i)^2}{\sum_{i=1}^{n}(measured\ value_i - mean\ value)^2} \quad (12)$$

$$RMSE = \sqrt{\frac{\sum_{i=1}^{n}(predicted value_i - measured value_i)^2}{n}} \quad (13)$$

$$MAE \frac{\sum_{i=1}^{n}|predicted\ value_i - measured\ value_i|}{n} \quad (14)$$

Measured value, measured value, predicted value by numerical model, predicted value, number of experiments, n, and average data, mean value, are defined in equations12, 13, and 14.

3. Results and discussion

Using drawn streamlines, the dimensions of the separated area in the main channel and the lateral intake were obtained and tabulated in Tables 1 and 2. The sizes are related to the separated area in depths of 3, 6, and 12 cm above the canal bed for all modes. Width and length of the separated area in the main channel and the lateral intake are depicted by cm in Tables 1 and 2, respectively. Laboratory results are given in the last rows of each table. With respect to comparing the laboratory results related to the width and length of the separated area in the main channel and the lateral intake, the less the discharge ratio, the more the amount of flow separation in the lateral intake.

When the discharge of lateral intake is low, the cross-sectional area of the lateral intake along with the constriction resulted from the separation can pass the flow. The separated area is in the form of a cone, where the closer one gets to the water surface, the more increase in volume of this combination and extension of the separated area. However, by increasing the discharge ratios, streamlines redirect, so that by reducing the amount of separation, lateral intake width can pass from discharge, and therefore the dimensions of the separation area will be smaller.

Table 1. Separated area length in the main channel and the intake

Turbulent model	Discharge ratio in depth 3,6, and 12 cm above canal bed																							
	0.2						0.4						0.6						0.8					
	3		6		12		3		6		12		3		6		12		3		6		12	
	M.c[1]	I[2]	M.c.	I	M.c.	I	M.c.	I	M.c.	I	M.c.	I	M.c.	I	M.c.	I	M.c.	I	M.c.	I	M.c.	I	M.c.	I
Prandtl mixing length	0	26.5	0	26.7	0	39.9	0	39.3	0	45.8	0	38.4	6.2	0	0	0	0	8.3	0	13.2	0	15.6	0	18.9
Turbulent energy	0	57.2	0	51.5	0	49.3	0	67.4	0	60.1	0	25.3	0	31.1	0	33.5	0	34.2	58.7	45.1	47.7	46.5	0	48.4
k-ε	0	40.7	0	82.1	0	84.5	0	41.3	0	46.7	0	48.5	0	28.2	0	31.4	22	41.6	12.3	46.4	9.1	48.7	14.3	62.6
RNG	0	36.6	0	58.3	0	62.5	0	49.6	4.5	52.2	0	56.9	10.2	45.4	10.7	56.8	0	61.5	6.4	51.3	8.7	52.9	10.1	58.5
Large eddy	0	11.2	0	11.8	0	18.8	6.2	20.1	10	21.4	11.2	20.8	14.3	16.5	14.3	17.7	15.9	15.6	15.1	36.7	25	12.2	29.3	50.1
Laboratory results	0	35.9	0	57.5	0	65.1	10.3	55	11.2	56.5	12.5	62.5	7.5	50	8.7	57.3	10.6	65	8.7	50	10.4	55	11.2	62.5

Table 2. Separated area width in the main channel and the intake

Turbulent model	Discharge ratio in depth 3,6, and 12 cm above canal bed																							
	0.2						0.4						0.6						0.8					
	3		6		12		3		6		12		3		6		12		3		6		12	
	M.c.	I	M.c.	I	M.c.	I	M.c.	I	M.c.	I	M.c.	I	M.c.	I	M.c.	I	M.c.	I	M.c.	I	M.c.	I	M.c.	I
Prandtl mixing length	0	6.4	0	6.7	0	6.1	0	8.2	0	8.3	0	8.6	2	0	0	0	0	4.9	0	3.1	0	4.4	0	4.3
Turbulent energy	0	11.7	0	11.2	0	12.5	0	11.3	0	11.6	0	7.9	0	5.8	0	6.7	0	6.4	23.7	0	18	2.4	0	2.1
k-ε	0	14.2	0	13.4	0	18.7	0	8.1	0	10.2	0	7.3	0	6.1	0	7.4	1.6	9.2	7	18.1	3.4	10	6.7	18.2
RNG	0	16.5	0	15.9	0	18.2	0	10	1.5	11.4	0	11.8	3.4	7.9	2.3	10.9	0	16.8	1.9	9.3	2.1	13.7	3.5	14.1
Large eddy	0	4.1	0	4.8	0	7.2	4	10.6	6.3	8.7	4.1	7.4	15.6	12.3	4.3	10.2	9.5	10.6	14.8	9.2	14.6	11.2	13.7	9.3
Laboratory results	0	15.2	0	16.1	0	19.7	22	13.7	2.5	16.2	3.2	17.5	1.5	9.7	1.7	11.5	2.2	15	1.5	11.5	1.7	12.5	2.3	12.7

[1]Main Channel
[2]Intake

Figure 18 compares the results between the laboratory observations and the predicted ones by the numerical model for all of the discharge ratios in the turbulence model RNG. The cores are according to cm.

The 45° line represents the perfect agreement of the laboratory observations and the values predicted by the numerical model.

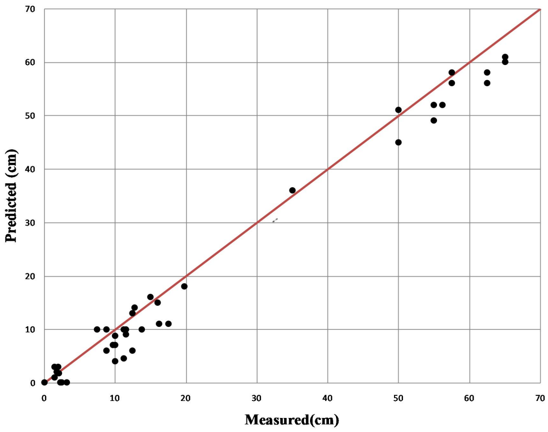

Fig.18. Comparison of the results between the laboratory observations and the values predicted by the numerical model over all of the discharge ratios in RNG turbulent model

In comparing results between the experimental observations and the predicted values by the numerical model correlation coefficient, root mean square error, and mean absolute error were obtained as of 0.97, 3.16 cm, and 2.3 cm, respectively.

Figure 19 compares the results between the laboratory observations and the values predicted by the numerical model, in all of the discharge ratios in the turbulence model k-ε.

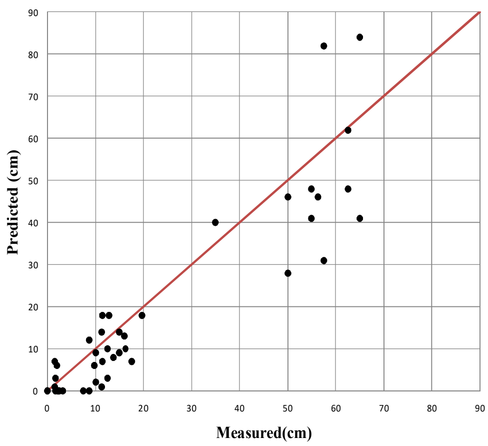

Fig. 19. Comparison of the results between the laboratory observations and the values predicted by the numerical model, over all of the discharge ratios in k-ε turbulent model

In comparing the results of the laboratory observations and the predicted values of the numerical model, correlation coefficient was 0.81, root mean square error was 9.37 cm, and mean absolute error was obtained 6.4 cm.

Figure 20 compares the results between the experimental observations and the predicted values of the numerical model for all of the discharge ratios in the large eddy turbulence model.

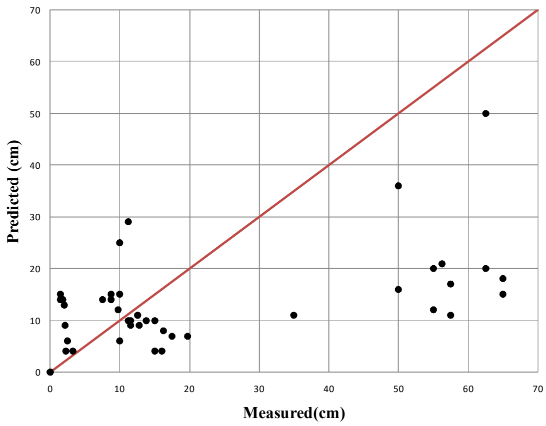

Fig. 20. Comparison of the results between the laboratory observations and the values predicted by the numerical model, over all of the discharge ratios in large eddy turbulent model

In comparing the results of the laboratory observations and the values predicted by the numerical model, correlation coefficient of 0.17, root mean square error of 19.84 cm, and mean absolute error of 13.24 cm were obtained.

Figure 21, compares the results between the laboratory observations and the values predicted by the numerical model, in all of the discharge ratios in the Prandtl mixing length turbulence model.

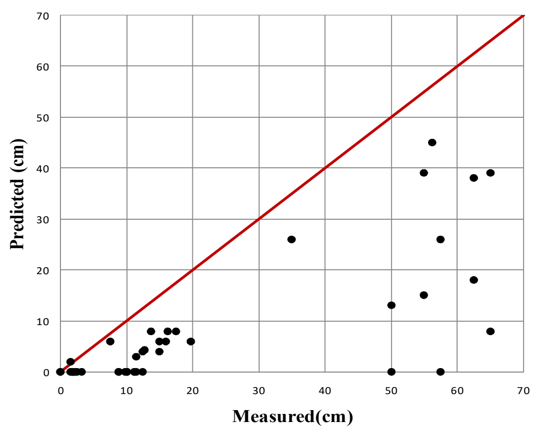

Fig. 21. Comparison of the results between the laboratory observations and the predicted values of the numerical model, over all of the discharge ratios in Prandtl mixing length turbulent model

In comparing the results of the laboratory and the predicted observations, correlation coefficient of 0.18, root mean square error of 19.77 cm, and mean absolute error of 12.91 cm were achieved.

Figure 22 compares the results between the laboratory observations and the values predicted by the numerical model, in all of the discharge ratios for the kinetic energy turbulence model.

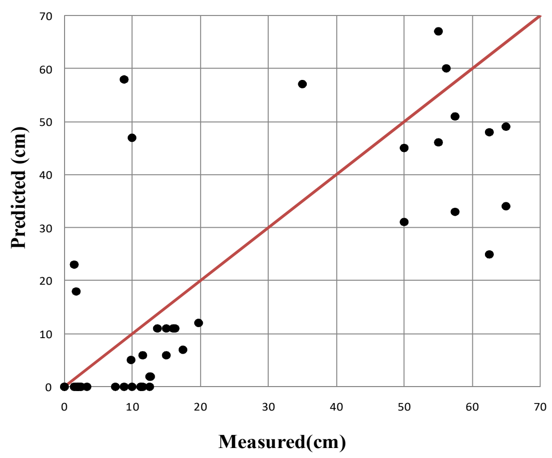

Fig. 22. Comparison of the results between the laboratory observations and the predicted by the numerical model, over all of the discharge ratios in Turbulent energy turbulent model

In comparing the results of the laboratory observations and the values predicted by the numerical model, correlation coefficient of 0.53, root mean square error of 14.87 cm, and mean absolute error of 10.38 cm, were obtained.

4. Conclusion

In this research, the width and length of the separated area in 90 degrees intake were predicted using Flow-3D numerical model for various discharge ratios and 5 turbulence models at 3, 6, and 12 cm flow depth above canal bed. The results were then compared with the observations of the physical model.

In order to prepare the channel geometry, AutoCAD software was used. Using the obtained velocity components from Flow-3D, model streamlines were drawn for various turbulence models at different depths by Tecplot software. In comparing the results between the laboratory observations and the values predicted by numerical models for all of the discharge ratios, RNG turbulence model had the highest precision in prediction and the large eddy turbulence model had the lowest precision in predicting the separated areas dimensions.

RNG model with a correlation coefficient of 0.97, root mean square error of 3.16 cm, and mean absolute error of 2.3 cm had better prediction compared to the other turbulence models and the most difference in predicting the turbulence model of large eddy was achieved using correlation coefficient of 0.17, root mean square error of 19.84 cm, and mean absolute error of 13.24 cm.

5. References

Gohari, S. (2012). Laboratory investigation of separation line at the intake sand its relation to sediment control. 9th International Congress on Civil Engineering, Isfahan Univesity of Technology, Isfahan, Iran.

Issa, R.I., & Oliveira, P.J. (1994). Numerical prediction of phase separation in two-phase flow through T-junction. Computational and Fluids, 23(2):347-356.

Kasthuri, B.,& Pundarikanthan, N.V. (1987). Discussion on separation zone at open channel junctions. Journal of Hydraulic Engineering, 113(4):543-548.

Karami Moghaddam, M., & Keshavarzi, E. (2007). Investigation on flow pattern intheintakes of56and90 degreewithedged entrance. 3rd National Congress on Civil Engineering. 1-3 May 2007. University of Tabriz, Tabriz, Iran.

Karami Moghaddam, M. (2007). determination ofoptimumradiusof entrance of the intakes of56and90 degree. M.Sc. thesis, Faculty of agriculture, University of Shiraz.

Neary, V.S.,& Odgaard, A.J. (1993). Three dimensional flow structure at open channel diversions. Journal of Hydraulic Engineering, 119(11):1223-1230.

Neary, V.S., & Sotiropoulos, F. (1996). Numerical investigation of laminar flows through 90-degree diversion of rectangular cross-section. Computational and Fluids, 25(2):95-118.

Neary, V.S. (1999). Three-dimensional numerical model of lateral-intake inflows. Journal of Hydraulic Engineering, 125(2):126-140.

Neary, V.S., Sotiropoulos, F., & Odgaard, A.J. (1999). Three-dimensional numerical model of lateral-intake inflows. Journal of Hydraulic Engineering, 125(2):126-140.

Ramamurthy, A.S., Junying Q.U.,& Diep, V.O. (2007). Numerical and experimental study of dividing open-channel flows. Journal of Hydraulic Engineering, 133(10):1135-1144.

Shettar, A.S., & Murthy, K.K. (1996). A numerical study of division of flow in open channels. Journal of Hydraulic Research, 34(5):651-675.

Shames, I.R. (1982). Mechanics of fluid, 2nd edition. McGraw-Hill international book company.

Seyedian, S.M., &Shafai Bajestan, M. (2008). Determination of the flow patternin lateral intakesusing mathematical models.3rd Conference on Water resources, 14-16 Oct. 2008. University of Tabriz, Tabriz, Iran.

Tataroglu, R.M., & Özgen, C. (2014). Numerical Investigation of Vortex Formation at Intake Structures using Flow-3D Software. Journal of Hydraulic Research, 31(4):41-45.

Wilcox, D.C. (1993). Turbulence Modeling for CFD. DCW Industries, La Canada, California.